pression represents the departure from classical sandwich beam theory. It is interesting to note that the maximum shear stress departure ratio depends only upon the single parameter $\lambda L/2$, whereas the bending stress and deflection departure ratios depend upon the geometric sandwich depth parameter h/t as well. A plot of Eq. (24) is presented in Fig. 2. Figures 3 and 4 show families of curves for Eqs. (25) and (26), respectively, for a wide range of values of h/t.

Uniform Short Beams

A useful extrapolation of the present results to homogeneous beams is also possible. Note that a homogeneous beam carries almost 80% of the bending moment in the outer two-fifths of the external fibers. The remainder, or three-fifths of the cross section, carries almost 90% of the entire shear. This suggests that we could approximate a uniform beam as a sandwich beam, of the type discussed here, with an h/t of 3. Setting $G/E^* = [2(1+\nu)]^{-1}$, we obtain

$$\lambda L/2 = 10.1\, L/(D\sqrt{1+\nu}) \tag{27}$$

where $D = h + 2t$, the entire beam depth.

From Figs. 2 and 3, we observe that, for $h/t \approx 3$, the simple beam theory shear and bending stress formulas are 99% accurate for $\lambda L/2 > 80$ and 40, respectively, and are applicable for deflections (Fig. 4) when $\lambda L/2 > 100$. Thus, for $\nu = 0.3$, the approximate length-to-beam-depth ratios required for the use of classical beam formulas are

$$\tau_{\substack{\text{uniform}\\\text{beam}}} = \tau_{\text{classical}} \quad \text{when} \quad L/D > 9$$

$$\sigma_{\substack{\text{uniform}\\\text{beam}}} = \sigma_{\text{classical}} \quad \text{when} \quad L/D > 5$$

$$w_{\substack{\text{uniform}\\\text{beam}}} = w_{\text{classical}} \quad \text{when} \quad L/D > 11$$

References

[1] Yu, Y.Y., "A New Theory of Elastic Sandwich Plates – One-Dimensional Case," *Journal of Applied Mechanics*, Sept. 1959, pp. 415-421.

[2] Hoff, N.J., *The Analysis of Structures*, Wiley, New York, 1956.

[3] Plantema, F.J., *Sandwich Construction*, Wiley, New York, 1966.

[4] Raville, M.E., "Deflections and Stresses in a Uniformly Loaded Simply Supported, Rectangular Sandwich Plate," Forest Products Lab., Rept. 1847, Dec. 1955.

[5] "Structural Sandwich Composites," Dept. of Defense, Washington, D.C., Military Handbook MIL-HDBK-23A, Dec. 1968.

Boundary-Value Problem of Configurations with Compressible Free Vortex Flow

Guenter W. Brune* and Paul E. Rubbert†
The Boeing Company, Seattle, Wash.

Introduction

IN this Note, a self-consistent formulation of the compressible boundary-value problem of configurations with leading-edge vortex separation is presented. Based on the assumption that the compressible flowfield is governed by the linearized potential equation, the limitations imposed on mass flux and pressure formulations are examined thoroughly. The result of this investigation is utilized to formulate the stream surface boundary condition and the zero pressure jump condition of compressible free vortex flows in a manner consistent with the linear potential equation. It is shown further that, in the subsonic flow domain, the compressible nonlinear boundary-value problem can be transformed completely into an equivalent nonlinear incompressible problem by application of the Goethert rule. Previous solutions to the linearized compressible flow equation applied to free vortex flows either utilized a linearized pressure equation[1] or followed a completely different line of thought dictated by the chosen solution method.[2]

A few numerical calculations of subsonic leading-edge vortex flows about planar wing geometries support the theoretical result. The sample calculations were performed using a modified version of a previously developed method[3] of predicting incompressible flow about three-dimensional configurations with vortex separation from sharp-edged wings. The method utilizes an inviscid flow model in which the wing and the rolled-up primary vortex sheets are represented by piecewise continuous quadratic doublet sheet distributions. Computational experience with this method has shown that it is capable of producing accurate predictions of detailed surface pressure distributions, forces, and moments. The compressibility corrections discussed in this Note extend the range of applicability of the method to higher subsonic Mach numbers.

Received April 13, 1977; revision received July 5, 1977.

Index categories: Aerodynamics; Subsonic Flow; Computational Methods.

*Specialist Engineer. Member AIAA.

†Supervisor, Aerodynamic Analysis Group. Associate Fellow AIAA.

Choice of a Linear Potential Equation

The familiar linear equation of the perturbation velocity potential ϕ

$$(1 - M_\infty^2)\phi_{xx} + \phi_{yy} + \phi_{zz} = 0 \tag{1}$$

is chosen to govern the compressible flowfield. The equation is written in wind-fixed Cartesian coordinates x, y, z, whose positive x axis points in the direction of the freestream velocity U_∞. The symbol M_∞ denotes the Mach number of the undisturbed freestream.

The choice of this linear equation is a matter of convenience and computational efficiency, since it allows the application of the superposition principle and consequently the use of aerodynamic panel methods. However, the equation imposes certain well-known restrictions[4] on the analysis and, in particular, excludes the transonic speed regime from the theoretical treatment. The limitations imposed by this equation on the formulations of mass flux vector and pressure now will be investigated.

With the help of the continuity equation for steady flow, $\text{div}(\rho V) = 0$, one can show[4] that the following lowest-order approximation to the mass flux vector (ρV) is a consequence of the choice of Eq. (1):

$$\rho V = \rho_\infty \{ [U_\infty + (1 - M_\infty^2) u] e_x + v e_y + w e_z \} \tag{2}$$

The symbols e_x, e_y, e_z are the unit vectors of the coordinate system x, y, z. The components of the perturbation velocity $\nabla\phi$ in these coordinates are u, v, w. The symbols U_∞ and ρ_∞ denote the velocity magnitude and the density of the freestream, respectively. Comparison of the mass flux vector given by Eq. (2) with the velocity vector

$$V = (U_\infty + u) e_x + v e_y + w e_z \tag{3}$$

shows that the mass flux vector, postulated by the linear theory equation (1) to exist, is no longer parallel to the velocity vector if one chooses to retain the term involving u in the definition of the vector. In classical linear theory, this term is neglected as being of higher order; however, if one postulates the use of nonlinear boundary conditions, then the term involving u must be considered. An approximation to the pressure p which is consistent with Eq. (1) can be derived from the momentum equation for steady inviscid flow:

$$(\rho V)\cdot \mathrm{grad}\, V + \mathrm{grad}\, p = 0 \tag{4}$$

Introducing the mass flux vector as given by Eq. (2), the resulting equation for the pressure coefficient c_p takes the form

$$c_p = 1 - \frac{V\cdot V}{U_\infty^2} + M_\infty^2 \frac{u^2}{U_\infty^2}, \qquad c_p = \frac{p - p_\infty}{(\rho_\infty/2)U_\infty^2} \tag{5}$$

which is known in the literature as the quadratic approximation to Bernoulli's equation.[4]

Formulation of the Boundary Conditions

It is postulated at the outset that exact stream surface boundary conditions can be stated as

$$(\rho V)\cdot n = 0 \tag{6}$$

i.e., the mass flux vector must be tangential to all solid surfaces of the configuration, to the vortex sheets separating from sharp wing edges, and to the wake. The symbol n denotes the normal vector of the configuration surface. Since the density ρ is a scalar, one is tempted to replace this mass flux boundary condition by the familiar velocity boundary condition, $V\cdot n = 0$. However, as shown earlier, the mass flux vector is not parallel to the velocity vector when retaining terms involving u, so that application of velocity boundary conditions would cause the surfaces of the configuration to generate or absorb mass. In view of this anomaly, the intended simplification obviously is not permitted.

The boundary condition (6) must be satisfied on both sides of a thin surface. It therefore is possible to introduce an average stream surface boundary condition

$$(\rho V)^s \cdot n = 0 \tag{7}$$

formulated in terms of the average mass flux vector $(\rho V)^s$, defined by

$$(\rho V)^s = \tfrac{1}{2}[(\rho V)_u + (\rho V)_l] \tag{8}$$

The subscripts l and u denote the lower and upper sides of a thin surface, respectively.

Free vortex surfaces, such as the primary vortex sheets and the wake, cannot sustain a pressure differential across them. This is the so-called zero pressure jump boundary condition, written as

$$\Delta c_p = c_{p_l} - c_{p_u} = 0 \tag{9}$$

Using the pressure formula (5), the boundary condition (9) can be specialized to

$$\Delta c_p = (2/U_\infty^2)(V^s \cdot V^D - M_\infty^2 u^s u^D) = 0 \tag{10}$$

where an average sheet velocity V^s and a velocity difference across the sheet V^D are defined by

$$V^s = \tfrac{1}{2}(V_u + V_l), \qquad V^D = V_u - V_l \tag{11}$$

with corresponding definitions of average and difference values of the perturbation velocity components. Noting that the averages of mass flux vector and velocity vector are related by

$$(\rho V)^s = \rho_\infty V^s - \rho_\infty M_\infty^2 u^s e_x \tag{12}$$

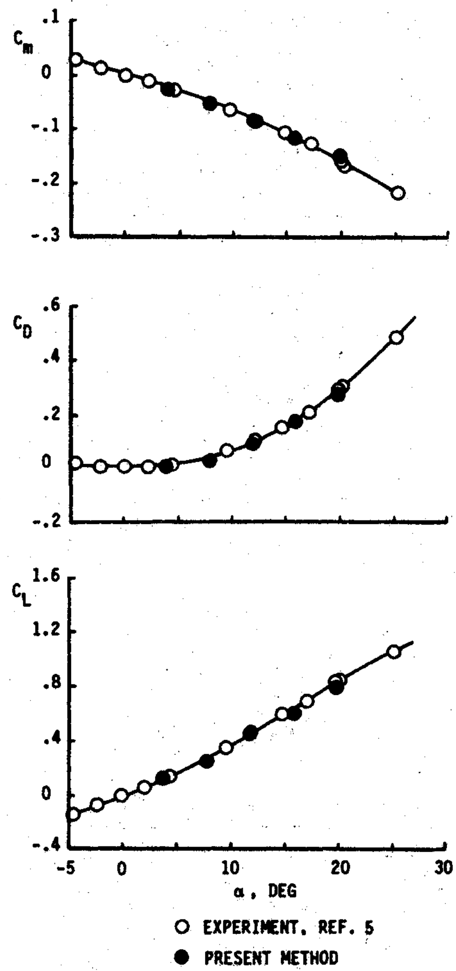

Fig. 1 Delta wing characteristics at $M_\infty = 0.8$, $AR = 1.15$.

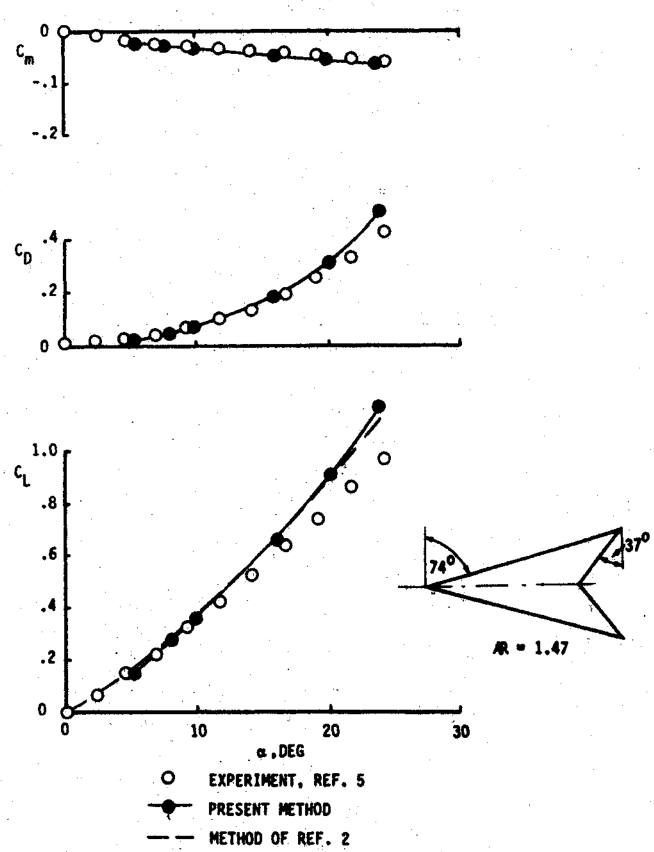

Fig. 2 Arrow wing results at $M_\infty = 0.6$.

one arrives at

$$\Delta c_p = (2/\rho_\infty U_\infty^2)(\rho V)^s \cdot V^D = 0 \tag{13}$$

So far, no distinction has been made between subsonic and supersonic speed regimes. Beginning with the next section, the discussion is restricted to the subsonic flow domain.

Application of the Goethert Rule

The boundary conditions of incompressible free vortex flow, which correspond to boundary conditions (7) and (13) of the compressible domain, read

$$V_i^s \cdot n_i = 0 \tag{14}$$

$$\Delta c_{p_i} = (2/U_\infty^2) V_i^s \cdot V_i^D = 0 \tag{15}$$

The subscript i denotes quantities in the incompressible flow domain.

The question now arises as to which, if any, of the various transformations that reduce the compressible potential Eq. (1) to Laplace's equation also reduce the boundary conditions of the compressible domain as given by Eqs. (7) and (13) to their equivalent form in the incompressible flow domain. It can be verified easily that the desired transformation is achieved by application of the following well-known version of the Goethert rule:

$$x_i = x/\beta,\ y_i = y,\ z_i = z,\ \phi_i = \beta\phi,\ \beta = \sqrt{1-M_\infty^2} \tag{16}$$

The freestream velocity is kept fixed during the transformation, but the angle of attack changes as $\tan\alpha_i = \beta \tan\alpha$. By application of the Goethert rule to Eq. (5), one can show further that the pressure distributions of both flow domains are related by

$$c_p = c_{p_i}/\beta^2 \tag{17}$$

where c_{p_i} is obtained from Bernoulli's equation.

It should be emphasized that boundary conditions (14) and (15) of the incompressible flow domain are applied on the surface $z_i = f_i(x_i, y_i)$, and that boundary conditions (7) and (13) of the compressible domain are applied on the surface $z = f(x,y)$, where

$$f_i(x_i, y_i) = f(\beta x_i, y_i) \tag{18}$$

Numerical Results

The accuracy of the Goethert rule used in combination with exact boundary conditions involving the mass flux vector was investigated numerically by calculating the subsonic flow about planar wing geometries over a wide range of angles of attack. The wing planforms were transformed according to Eq. (16), and the resulting incompressible flow problems were solved using a modified version of the numerical technique of Ref. 3. The computed compressible values of lift coefficient c_L, drag coefficient c_D, and pitching moment coefficient c_m are compared in Figs. 1 and 2 with experimental data of Ref. 5. The coefficients are referred to wing area, freestream dynamic pressure, and mean aerodynamic chord. The pitching moment reference axes of the delta wing and the arrow wing are located at 50% and 64.5% root chord, respectively. It is shown in Fig. 1 that the characteristics of the delta wing are very well predicted even at the extreme flight condition of 20 deg angle of attack and 0.8 freestream Mach number. Drag and pitching moment characteristics of the arrow wing are shown in Fig. 2 to be well predicted up to 20 deg angle of attack, although the lift is overpredicted at higher incidences. For comparison, theoretical data of the lift coefficient obtained from the leading-edge suction analogy of Polhamus[2] also are shown; the agreement with the theoretical results of the method reported in this Note is remarkable.

Acknowledgment

This research was supported partly by NASA Langley under Contract NAS1-13833 and partly by the Independent Research and Development Program of The Boeing Company. The authors wish to thank Forrester T. Johnson and Paul Lu of The Boeing Company for their support in generating some of the numerical results.

References

[1] Kandil, O. A., Mook, D. T., and Nayfeh, A. H., "Effect of Compressibility on the Nonlinear Prediction of the Aerodynamic Loads on Lifting Surfaces," AIAA Paper 75-121, Pasadena, Calif., Jan. 20-22, 1975.

[2] Polhamus, E. C., "Charts for Predicting the Subsonic Vortex-Lift Characteristics of Arrow, Delta, and Diamond Wings," NASA TN D-6243, 1971.

[3] Weber, J. A., Brune, G. W., Johnson, F. T., Lu, P., and Rubbert, P. E., "A Three-Dimensional Solution of Flows Over Wings with Leading Edge Vortex Separation," *AIAA Journal*, Vol. 14, April 1976, pp. 519-525.

[4] Ward, G. N., *Linearized Theory of Steady High-Speed Flight*, Cambridge University Press, London, 1955.

[5] Davenport, E. E., "Aerodynamic Characteristics of Three Slender Sharp-Edge 74° Swept Wings at Subsonic, Transonic, and Supersonic Mach Numbers," NASA TN D-7631, 1974.

Centroidal and Area Average Resistances of Nonsymmetric, Singly Connected Contacts

M. M. Yovanovich* and S. S. Burde†
University of Waterloo, Waterloo, Ontario, Canada

Introduction

It was demonstrated in a recent paper[1] that the normalized constriction resistance $\lambda\delta R$ is approximately equal to the value 5/9 and 84% of this value when δ is chosen to be the square root of the contact area and when the resistance in the first instance is based upon the centroid temperature and in the second upon the area average temperature. This remarkable fact was observed for a set of singly connected, symmetric planar contacts of the form $(x/a)^n + (y/b)^n = 1$, with $b = a$ subject to the same uniform heat flux. The geometric parameter n was allowed to range from $n = ½$ to $n = \infty$, thereby covering a variety of shapes which included astroids, a circle, a square, and near squares.

To determine whether the results of the symmetric study are general, three nonsymmetric shapes were examined. This Note describes the method used to obtain the temperature at arbitrary points and the centroidal temperature for a triangular contact, a semicircular contact, and an L-shaped contact. A numerical method was used to obtain the area average temperature of these contact areas.

Arbitrary and Area Average Temperatures

Triangular Contact Area

Figure 1 shows a singly connected, planar triangular contact area of base $2a$ and height $2b$ subjected to a uniform heat flux q. The half-space thermal conductivity is λ. The expression for the normalized resistance based upon the area

Received April 1, 1977; revision received July 11, 1977.

Index categories: Spacecraft Temperature Control; Heat Conduction; Thermal Modeling and Analysis.

*Professor, Thermal Engineering Group, Department of Mechanical Engineering. Associate Fellow AIAA.

†Graduate Research Assistant, Thermal Engineering Group, Department of Mechanical Engineering.